Central European Journal of Energetic Materials, **2013**, *10*(1), 17-36
ISSN 1733-7178

Synthesis, Crystal Structure, and Properties of a Novel, Highly Sensitive Energetic, Coordination Compound: Iron (II) Carbohydrazide Perchlorate

Rui LIU, Zunning ZHOU, Shuyuan QI, Li YANG, Bidong WU, Huisheng HUANG and Tonglai ZHANG*

State Key Laboratory of Explosion Science and Technology, Beijing Institute of Technology, Beijing 100081, China
**E-mail: ztlbit@bit.edu.cn*

Abstract: A single crystal of iron (II) carbohydrazide perchlorate $[Fe^{II}(CHZ)_3](ClO_4)_2$ (FeCP), a novel, lead-free, energetic coordination compound, was synthesized and its structure determined by X-ray single crystal diffraction for the first time. The crystal belongs to the monoclinic system *P*2(1)/n space group, with $a = 1.0066(2)$ nm, $b = 0.8458(2)$ nm, $c = 2.1194(4)$ nm, $\beta = 100.693(3)°$ and $Z = 4$. The central Fe(II) ion is coordinated to three bidentate carbohydrazide units through the carbonyl oxygen atom and an amino nitrogen atom, forming a six-coordinated, non-centrosymmetric complex cation. The thermal analyses by differential scanning calorimetry and thermogravimetry show that the onset temperature of thermal decomposition (152.7 °C) and the critical temperature of thermal explosion of FeCP (161.2 °C) are both much lower than those of other transition metal carbohydrazide perchlorate compounds, and also those of some other primary explosives in service. FeCP has a high enthalpy of combustion, as measured by oxygen bomb calorimetry. The impact, friction and flame sensitivity tests indicate that FeCP is extremely sensitive and hazardous. Unexpected explosions occurred even during the operational processes. In order to explore the intrinsic cause of these explosions, theoretical calculations of the orbital energies were performed based on DTF. These results reveal that the impact sensitivity is positively correlated with the energy gap between HOMO and LUMO: the smaller energy gap results in the higher impact sensitivity.

Keywords: iron (II) carbohydrazide perchlorate, energetic material, high sensitivity, DFT, energy gap

Introduction

Iron and its salts are widely used in the chemical industry [1, 2], in biological engineering [3, 4] and in pharmaceutical development [5], and are also closely related to our daily life [6, 7]. In the field of energetic materials, iron, as an environmentally benign metal, is expected to allow lead-free, green, energetic coordination compounds to be prepared [8-11]. Much attention has been paid into selecting appropriate ligands and anions for iron to form high-energy compounds. Carbohydrazide (CHZ), as a polydentate azotic ligand, has aroused great interest in the design of eco-friendly, primary explosives [12-14]. Perchlorate is undeniably a competent oxidizer used in many solid propulsion systems with prominent explosive performance [15-18], though it poses environmental hazards and even threatens human health [19, 20]. The widely used ammonium perchlorate (AP), penta(ammine)(5-cyanotetrazolate-N^2) cobalt(III) perchlorate (CP) and tetra(ammine)di(5-nitrotetrazolate-N^2) cobalt(III) perchlorate (BNCP) have many desirable properties [21-23]. Many transition metal coordination compounds based on carbohydrazide perchlorate have been synthesized and intensively studied. Furthermore they exhibit excellent thermal stability and explosive performance, and have promising applications as lead-free primary explosives [24-29].

Unexpectedly, explosions occurred during the filtration and drying processes, when preparing the similarly-structured iron (II) carbohydrazide perchlorate (FeCP), even though no inappropriate operations were performed. The explosions even led to the destruction of laboratory equipment. This indicated that FeCP is most probably an extremely sensitive and hazardous material. Because iron is widely used in weapon and civil utensils in conjunction with explosives, these security problems aroused our considerable attention. FeCP may be much less stable than other transition metal carbohydrazide perchlorate compounds (MCPs). Study of unstable compounds helps to elucidate the fundamental properties affecting chemical stability, to avoid hazards during processing, and to explore their potential applications [30-32]. Therefore, it was relevant to investigate this novel, highly sensitive, energetic coordination compound FeCP, in order to reveal the inherent cause of the hazards and to prevent accidents and injuries. A single crystal of FeCP was prepared and examined by X-ray diffractometry and elemental analysis. Its thermal properties and sensitivity were also studied. Theoretical calculations of its orbital energies based on density functional theory (DFT) were performed and the results were compared with experimental data.

Experimental

General caution: FeCP is a very sensitive and very dangerous energetic material, tending to explode under only very slight stimulus even in the wet state. The appropriate safety precautions, such as safety glasses, face shield, leather coat and ear plugs, must be used during processing.

Synthesis on a small scale

All chemical reagents were commercially supplied of analytical grade purity and were used without further purification.

FeCP was synthesized on a small scale to avoid hazards according to the scheme as shown in Figure 1.

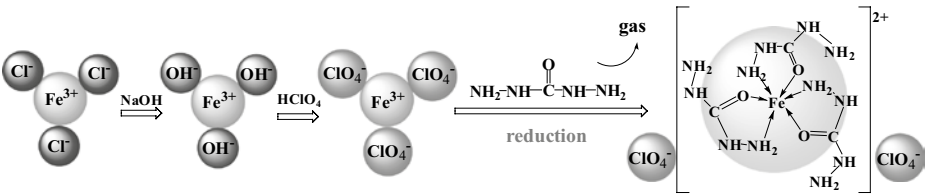

Figure 1. Schematic synthesis of FeCP.

A flocculent precipitate of $Fe(OH)_3$ was prepared by dropping NaOH solution (12 ml, 6 mmol) into $FeCl_3$ solution (4 ml, 2 mmol). After vacuum filtration and washing, the purified $Fe(OH)_3$ precipitate was dissolved in $HClO_4$ solution (6 ml, 6 mmol) with stirring, the solution was filtered and diluted to 10 ml, to obtain a solution of $Fe(ClO_4)_3$ (iron (III) perchlorate). A solution of carbohydrazide CHZ was obtained by dissolving CHZ (0.72 g, 8 mmol) in deionized water (50 ml), and then heating to 65 °C in a water bath. The $Fe(ClO_4)_3$ solution was added dropwise with stirring to the CHZ solution during 30 min. The mixed solution was kept stirring at 65 °C for 15 min, and was then cooled to room temperature. NB, this solution frequently produced an explosive crackling sound due to the constant release of bubbles during the reaction, which indicated that the product was very sensitive and dangerous. Finally light yellow, granular crystals were formed by slow evaporation in a culture box at 25 °C for 15 days. A single crystal of FeCP was carefully isolated from the solution by suction filtration, was washed twice with deionized water and once with ethanol, and then dried in an explosion-proof dryer. Elemental analysis was performed on a Flash EA 1112 fully-automatic trace element analyzer. The results show C (7.21%), H (3.53%), N (32.14%), compared with the theoretical values for $C_3H_{18}FeN_{12}O_{11}Cl_2$ of C (6.86%), H (3.43%), N (31.99%).

X-ray crystallography

The crystal structure analysis of FeCP was performed on a Rigaku AFC-10/Saturn 724$^+$ CCD X-ray single crystal diffractometer with graphite monochromated Mo-K_α radiation (λ = 0.71073 Å). A Lorentz polarization factor (*Lp* factor) and an empirical absorption correction were applied to the raw intensities. The structure was solved by direct methods using SHELXS-97 and refined by a full-matrix least squares on F^2 using SHELXL-97 [33]. All non-hydrogen atoms were obtained from the Fourier difference map and subjected to anisotropic refinement. All hydrogen atoms were generated geometrically and treated by a constrained refinement. The detailed crystallographic data and structure refinement is summarized in Table 1.

Table 1. Crystal data and structure refinement for FeCP

Empirical formula	$C_3H_{18}FeN_{12}O_{11}Cl_2$
Formula mass	525.04
Crystal system	Monoclinic
Space group	*P*2(1) / *n*
Temperature (K)	103(2)
a (nm)	1.0066(2)
b (nm)	0.8458(2)
c (nm)	2.1194(4)
β (°)	100.693(3)
Z	4
Cell volume (nm^3)	1.7731(6)
Density, calculated (g·cm^{-3})	1.967
Absorption coefficient (mm^{-1})	1.237
θ range for data collection (°)	3.1~27.5
h, *k* and *l* range	-12 to 13, -10 to 10, -24 to 26
Reflections measured	13488
Independent reflections (R_{int})	3938 (R_{int} = 0.029)
Goodness-of-fit on F^2	0.999
Final R_1 *and* wR_2 [$I>2\sigma(I)$][a]	R_1 = 0.0336, wR_2 = 0.0809

[a]$w=1/[\sigma^2(F_o^2)+(0.0415p)^2+1.8900p]$ where $p=(F_o^2+2Fc^2)/3$

Instruments and measurements

Differential scanning calorimetry (DSC) was carried out on a Pyris-1 differential scanning calorimeter (Perkin-Elmer, USA). The sample (about 0.2 mg, pure powder) was placed in an aluminum crucible in static air and heated at 10 °C·min^{-1}.

Thermogravimetric analysis (TGA) was performed on a Pyris-1 thermogravimetric analyzer (Perkin-Elmer, USA) at a heating rate of 10 °C·min^{-1} in a platinum crucible. The atmosphere was dynamic dry nitrogen at a flow rate of 20 ml·min^{-1}.

A Parr-6200 bomb calorimeter (static jacket) equipped with a 6510 water handling system and a Parr-1104 high strength bomb for the combustion of highly energetic materials was employed to determine the combustion enthalpy of FeCP. The calorimeter was calibrated by the combustion of certificated benzoic acid (about 1.0 g, pellet) in an oxygen atmosphere at a pressure of 3.10 MPa. The sample (about 0.5 g, pure powder) was placed in the combustion cage, and then ignited by the heating thread in a 3.10 MPa atmosphere of pure oxygen. The value of the combustion energy was obtained as the average of eight replicate measurements with the standard deviation calculated as a measure of experimental uncertainty.

All of the sensitivity tests were performed according to the standard methods [34-36]. The impact sensitivity was determined by the fall-hammer method, the friction sensitivity by the MGY-1 pendulum friction sensitivity apparatus, and flame sensitivity was ignited by a standard black powder pellet.

DFT calculations

The equilibrium geometry and the frontier molecular orbitals of FeCP were computed at the high spin state, using the spin-unrestricted HSE functional with the SDD pseudo potential basis set for the metal atoms and the 6-31G** basis set for the remaining atoms, by the GAUSSIAN software package program. Huang *et al.* has proved that the HSE functional performs best for reproducing the geometries of MCPs [37].

Results and Discussion

Structure descriptions

The molecular unit of FeCP, with the atom labelling scheme, is shown in Figure 2. Selected bond lengths and bond angles are listed in Table 2.

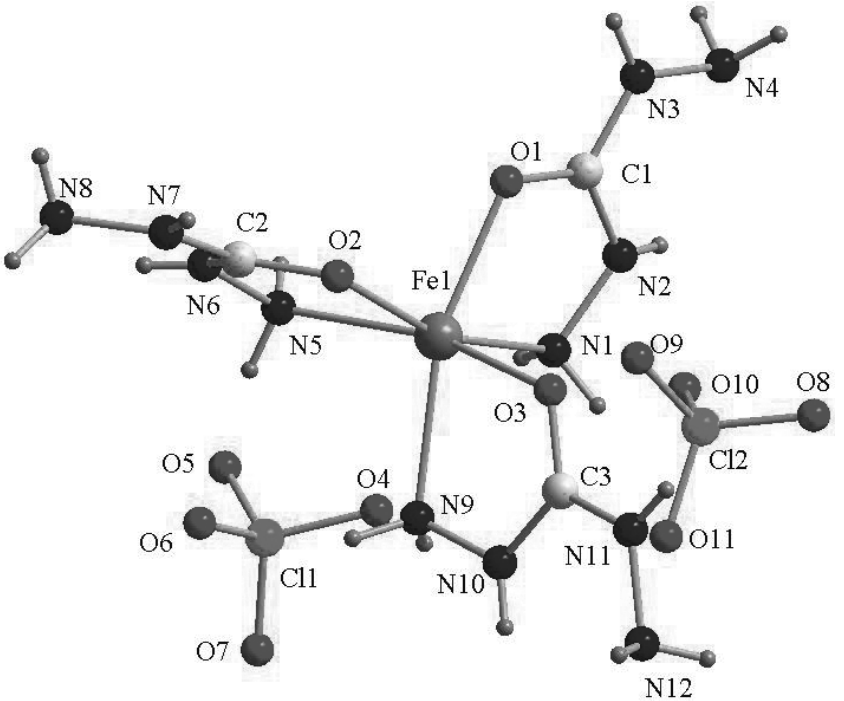

Figure 2. Molecular unit and labelling scheme for FeCP.

Table 2. Selected bond lengths and bond angles for FeCP

Bond lengths (nm)					
Fe1–O1	0.2080(2)	O2–C2	0.1262(3)	N11–N12	0.1409(4)
Fe1–O2	0.2124(2)	O3–C3	0.1254(3)	N6–C2	0.1342(3)
Fe1–O3	0.2069(2)	N1–N2	0.1418(3)	N7–C2	0.1332(3)
Fe1–N1	0.2217(2)	N2–C1	0.1346(3)	N7–N8	0.1403(3)
Fe1–N5	0.2212(2)	N3–N4	0.1411(3)	N9–N10	0.1413(3)
Fe1–N9	0.2239(2)	N3–C1	0.1331(3)	N10–C3	0.1346(3)
O1–C1	0.1258(2)	N5–N6	0.1414(3)	N11–C3	0.1327(3)
Bond angles (°)					
O1–Fe1–O2	88.20(6)	O2–Fe1–N5	75.38(6)	N5–Fe1–N9	93.69(7)
O1–Fe1–O3	94.14(6)	O2–Fe1–N9	105.09(6)	Fe1–O1–C1	116.12(13)
O1–Fe1–N1	76.13(6)	O3–Fe1–N1	94.64(7)	Fe1–O2–C2	116.00(13)
O1–Fe1–N5	100.31(6)	O3–Fe1–N5	158.82(6)	Fe1–O3–C3	117.81(13)
O1–Fe1–N9	162.81(6)	O3–Fe1–N9	75.39(6)	Fe1–N1–N2	107.61(13)
O2–Fe1–O3	89.79(6)	N1–Fe1–N5	103.77(7)	Fe1–N5–N6	109.64(13)
O2–Fe1–N1	163.96(6)	N1–Fe1–N9	90.95(7)	Fe1–N9–N10	108.24(14)

The molecular unit comprises one iron cation Fe(II), three CHZ neutral molecules and two ClO_4^- anions. The central Fe(II) has sp^3d^2 hybridization and contributes six empty orbits to accommodate the lone pair electrons from the ligands. CHZ as a bidentate ligand is coordinated with Fe(II) by the carbonyl oxygen atom and a terminal amino nitrogen atom. Therefore, three CHZ molecules simultaneously coordinate with the central Fe(II) to form a six-coordinated, non-centrosymmetric octahedron. Such a distorted geometric configuration is attributed to the Jahn-Teller effect. Thus, the diazanyl (–NH–NH_2) and the carbonyl (=C=O) from CHZ combine with the Fe(II) to form a five-membered chelating ring (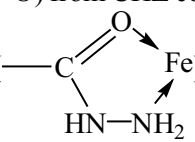). The bond lengths of Fe(II) to the coordinated O atoms (Fe–O) are approximately the same and those of Fe–N are also the same. However, the difference in bond length between Fe–O and Fe–N makes the ring exhibit a slightly distorted configuration. The bond lengths of Fe(II) to the six coordination atoms range from 0.2069(2) nm to 0.2239(2) nm, which indicates typical coordinated bonds. The bond angles of O–Fe–N from the three pentagonal rings are almost equiangular. The rings have very good co-planarity according to the equations of the least-squares planes listed in Table 3. The other diazanyl of each CHZ not involved in the formation of the chelate ring, stretches outside the ring to make the structure flexible and unstable. Two ClO_4^- anions as the outer anions, which are combined with the inner complex cation by electrostatic attraction and hydrogen bonds, make the molecular unit of FeCP relatively stable. The hydrogen bond lengths and bond angles are listed in Table 4. N2–H2, N6–H6, N10–H10 can form the intramolecular hydrogen bonds with N4, N8, and N12 in the same carbohydrazide, respectively. All N–Hs of the carbohydrazide can form intramolecular hydrogen bonds or intermolecular hydrogen bonds with the O atoms of ClO_4^- in different molecular units. Thus ClO_4^- plays a vital role in the formation of the crystal structure of FeCP. The molecular units of FeCP are linked together into a three-dimensional network structure by the intramolecular and intermolecular bonds. The packing diagram of FeCP is presented in Figure 3.

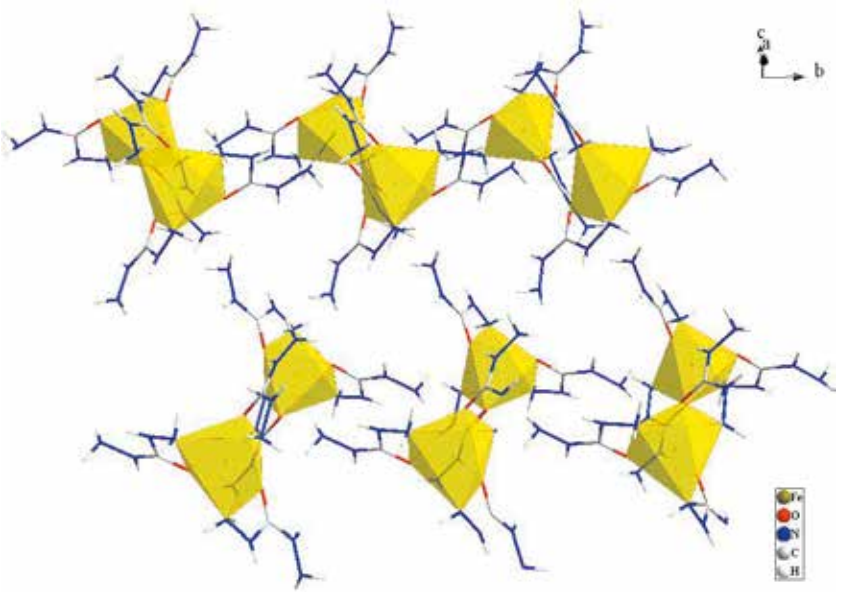

Figure 3. Packing diagram of FeCP in the crystal**.**

Table 3. Equations of least-square planes for the chelating rings

The chelating ring	Equation of least-square plane	Mean deviation from plane (nm)
Fe1,N9,N10,C3,O3	(-5.626)x+6.663y +(-3.192) z =(-3.2742)	0.00373
Fe1,N5,N6,C2,O2	5.996x+6.781y +(-1.321) z=2.4941	0.00281
Fe1,N1,N2,C1,O1	(-0.723)x+2.493y + 20.128z=12.6138	0.00631

Table 4. Hydrogen bond lengths and bond angles for FeCP

D–H···A	d(D–H) (nm)	d(H···A) (nm)	d(D···A) (nm)	∠(DHA) (°)
N1–H1A···O8	0.87(3)	2.25(3)	3.093(3)	162(3)
N1–H1B···O9	0.86(3)	2.53(3)	3.040(3)	119(2)
N1–H1B···O6	0.86(3)	2.45(3)	3.099(3)	133(3)
N2–H2···N4	0.80(3)	2.35(3)	2.657(3)	104(3)
N3–H3···O11	0.85(3)	2.21(3)	3.063(3)	176(3)
N4–H4A···O3	0.89(3)	2.32(3)	3.119(3)	150(3)
N4–H4B···O2	0.90(3)	2.18(3)	3.064(3)	170(3)
N5–H5A···O6	0.81(3)	2.58(3)	3.214(2)	136(3)
N5–H5B···O6	0.88(3)	2.14(3)	3.010(3)	172(3)

N6–H6···N8	0.76(3)	2.36(3)	2.634(3)	103(2)
N6–H6···O11	0.76(3)	2.58(3)	3.253(3)	149(2)
N7–H7···O10	0.85(3)	2.26(3)	3.060(4)	158(3)
N8–H8A···O7	0.80(3)	2.46(3)	3.038(3)	130(2)
N8–H8A···O1	0.80(3)	2.35(3)	2.993(3)	139(2)
N8–H8B···O7	0.89(3)	2.47(3)	3.082(3)	127(2)
N9–H9A···O4	0.87(3)	2.32(3)	3.061(3)	143(2)
N9–H9B···O5	0.89(3)	2.25(3)	3.069(3)	152(3)
N10–H10···O8	0.81(3)	2.26(3)	3.010(3)	155(3)
N10–H10···N12	0.81(3)	2.34(3)	2.661(3)	105(2)
N11–H11···O2	0.78(3)	2.17(3)	2.948(3)	176(3)
N12–H12A···O11	0.85(5)	2.54(5)	3.303(4)	150(4)
N12–H12B···O4	0.82(4)	2.38(4)	3.052(3)	140(4)

Thermal analyses

DSC and TG experiments were performed to investigate the thermal decomposition characteristics of FeCP. The DSC and TG curves of FeCP at a heating rate of 10 $^{\circ}C \cdot min^{-1}$ are shown in Figures 4 and 5 respectively.

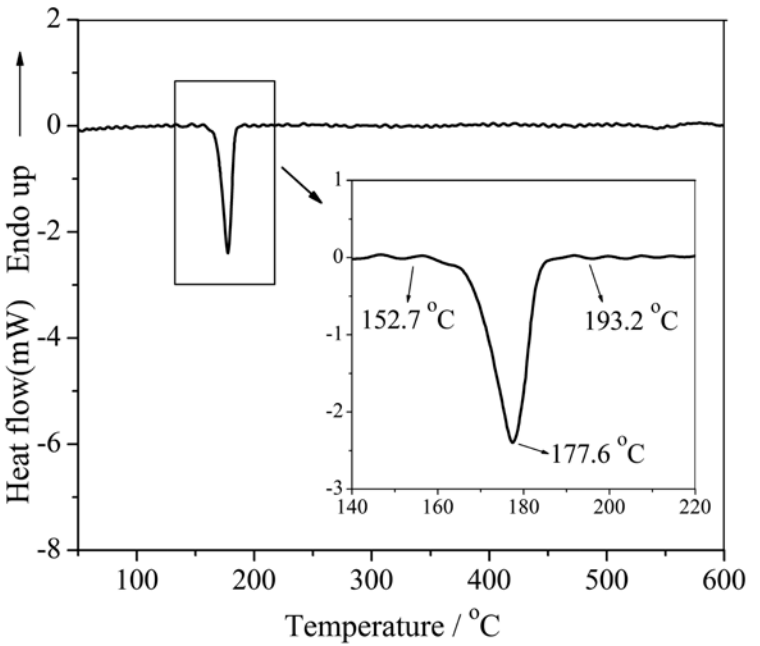

Figure 4. DSC curves of FeCP at a heating rate of 10 °C·min^{-1}.

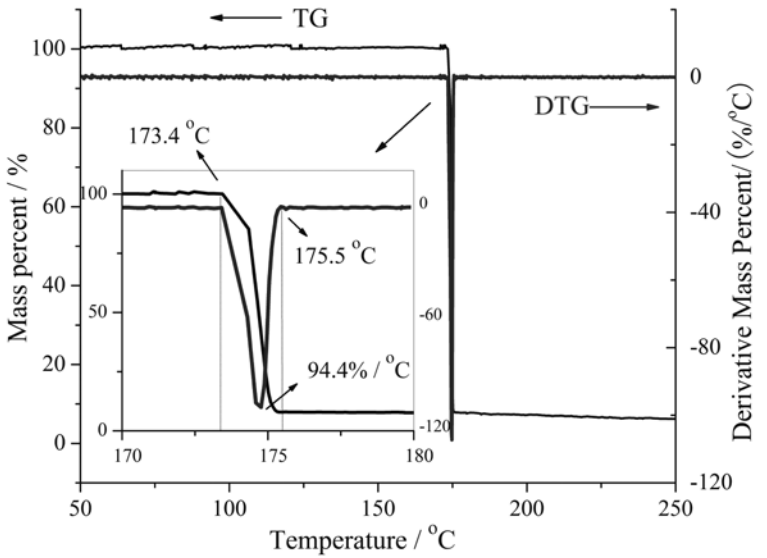

Figure 5. TG-DTG curves of FeCP at a heating rate of 10 °C·min^{-1}.

The DSC curve of FeCP shows only one exothermic peak in the temperature range 152.7-193.2 °C, with a peak temperature of 177.6 °C. Correspondingly, the TG–DTG curve exhibits a single-step, intense mass loss of 92.2 % from 173.4 °C to 175.5 °C with the maximum mass loss rate of 94.4%·°C^{-1}. The thermal behaviour reveals that FeCP is unstable at temperatures higher than 152.7 °C. Once the ambient temperature reaches the decomposition temperature, FeCP immediately explodes.

The critical temperature of thermal explosion (T_b) is an important indicator for the evaluation of the thermal safety of energetic materials. The method of calculation of T_b by DSC is as follows [38, 39]:

$$T_{ei} = T_{eo} + a\beta_i + b\beta_i^2 + c\beta_i^3 \tag{1}$$

$$T_b = \frac{E - \sqrt{E^2 - 4ERT_{eo}}}{2R} \tag{2}$$

where β_i is the heating rate, K·min^{-1}, T_{eo} is the extrapolated onset temperature in the DSC curve under linear temperature increase conditions when β_i tends to zero, K. T_{ei} is the extrapolated onset temperature obtained from the DSC curve with the heating rate β_i, K.

The linear equation, Eq. (1), can be defined using four groups of T_{ei} and β_i,

where β_i equals 5, 10, 15, 20 K·min^{-1}. As β_i tends to zero, the value of T_{ei} equals the value of T_{eo}. E is the activation energy which can be obtained using the same DSC analyses with Kissinger's method or Ozawa's method. The data of β_i, T_{ei} and the calculated T_{eo}, E and T_b values obtained from the DSC curves of MCPs are all listed in Table 5.

Table 5. Data of β_i, T_{ei} and the calculated T_{eo} and E values obtained from DSC curves

Compound	β (K·min^{-1})	T_{ei} (K)	T_{eo} (K)	E (J·mol^{-1})	T_b (K)
MnCP	5	551.9	534.6	133802.21	553.6
	10	565.0			
	15	573.5			
	20	577.0			
FeCP	5	408.5	422.1	125783.24	434.4
	10	419.2			
	15	424.4			
	20	429.8			
CoCP	5	556.9	521.5	177255.95	534.9
	10	569.2			
	15	571.5			
	20	576.9			
NiCP	5	575.7	556.9	137095.58	577.1
	10	583.2			
	15	588.9			
	20	602.3			
ZnCP	5	561.8	552.3	143808.62	571.2
	10	572.3			
	15	581.3			
	20	586.3			
CdCP	5	548.9	523.8	158124.06	539.1
	10	561.1			
	15	566.3			
	20	570.4			

The onset temperature of thermal decomposition (T_o) is another decisive factor for the thermal stability of a material. The T_o of FeCP is much lower than those of other MCPs (as Table 6 shows). FeCP is therefore the most thermally unstable compound of the MCP series.

Table 6. Thermal properties and sensitivity performances of MCPs

Compound	T_0 (°C)	T_b (°C)	Impact sensitivity $h_{50\%}$ (cm)	Friction sensitivity (%)	Flame sensitivity $h_{50\%}$ (cm)	Calculated energy gap (eV)
MnCP	270.5	280.4	28.1	60	no ignition	/
FeCP	152.7	161.2	9.6	98	explosion	4.44
CoCP	250.4	261.7	11.9	73	no ignition	4.87
NiCP	296.8	303.9	12.5	26	12.6	5.91
ZnCP	278.1	298.0	29.2	8	14	6.33
CdCP	258.2	265.9	24.5	40	no ignition	6.21

Determination of the enthalpy of combustion

The constant-volume combustion energy was determined using a Parr 6200 oxygen bomb calorimeter. The average combustion energy (Q_v) of FeCP was calculated as –4.652 ± 0.002 MJ·kg^{-1} by at least three replicate tests.

The complete combustion equation is shown below:

$$C_3H_{18}FeN_{12}O_{11}Cl_2(s) + \frac{11}{4}O_2(g) = \frac{1}{2}Fe_2O_3(s) + 3CO_2(g) + 9H_2O(l) + Cl_2(g) + 6N_2(g)$$

The enthalpy of combustion was calculated:

$$\Delta H = Q_p = Q_v + \Delta nRT = -4.688 \pm 0.002 \text{ MJ·kg}^{-1}$$

The enthalpy of combustion of FeCP is almost three times of that of LA (lead azide) (-1.5 MJ·kg^{-1}), and is also much higher than that of CdCP (-3.9 MJ·kg^{-1}) [40].

Sensitivity tests

FeCP demands the utmost care in handling.

The impact sensitivity was determined using a fall-hammer apparatus. FeCP (20 mg) was placed between two steel poles and hit with a 0.8 kg drop hammer from a starting height of 25 cm. The 50% firing height ($h_{50\%}$) of FeCP was 9.5 cm.

The friction sensitivity was determined using a pendulum apparatus. FeCP (20 mg) was compressed between two steel poles with mirror surfaces at a pressure of 1.23 MPa and then hit with a 1.5 kg hammer at 70° relative to the horizontal. The firing rate of FeCP was 98%.

The flame sensitivity was determined by the standard method in which the sample was ignited by a standard black powder pellet. FeCP (20 mg) was compacted into a copper cap under a pressure of 39.23 MPa before being ignited

by a standard black powder pellet. However, it was very difficult to complete this test because FeCP exploded unexpectedly during the pressing process.

The obvious difference between FeCP and the other MCPs is its sensitivity [25, 41-43]. The sensitivity performances of the MCPs are all shown in Table 6. FeCP has the highest sensitivity amongst these MCPs. Compared with the widely used CP, BNCP and LA [23, 43, 44], FeCP is the most highly sensitive (see Table 7). All of the above results indicate that FeCP is extremely sensitive to external mechanical stimuli. FeCP must be treated with utmost caution.

Table 7. Thermal properties and sensitivity performances of FeCP and other primary explosives

Compound	T_0 (°C)	Impact sensitivity $h_{50\%}$ (cm)	Friction sensitivity (%)	Flame sensitivity $h_{50\%}$ (cm)
FeCP	152.7	9.6	98	Explosion
CP	305.0	13.3	0	0
BNCP	266.2	10.6	24	80
LA	334.4	/	64	8

Correlation of energy gap with impact sensitivity

WHY is FeCP so sensitive? Because macroscopic behavior is ultimately controlled by microscopic properties [45-47], the essence of the sensitivity can be explored by theoretical calculations at the molecular level. Gilman [48-51] has confirmed that the energy gap (HOMO–LUMO) plays an important role in mechanically activated detonation. Therefore, the correlation of the energy gap with the impact sensitivity was investigated by DFT.

The error analyses of the bond lengths and bond angles from the experimental and theoretical geometries of FeCP are given in Table 8. The optimized geometry of FeCP closely matches the experimental result, which demonstrates the precision of the HSE functional with the 6–31G** basis set.

Table 8. Bond lengths and bond angles from the experimental and theoretical geometries of FeCP

Bond	Experimental (nm)	Theoretical (nm)	AE	RE
Fe1–O1	0.2080(2)	0.2015	0.0065	0.0313
Fe1–O2	0.2124(2)	0.2031	0.0093	0.0438
Fe1–O3	0.2069(2)	0.1994	0.0075	0.0363
Fe1–N1	0.2217(2)	0.2038	0.0179	0.0808
Fe1–N5	0.2212(2)	0.2053	0.0159	0.0719
Fe1–N9	0.2239(2)	0.2045	0.0194	0.0867
MAE: 0.1275	SE: 0.1376	MRE: 0.0585		
Angle	Experimental (°)	Theoretical (°)	AE	RE
O1–Fe1–N1	76.13(7)	82.069	5.932	0.0779
O2–Fe1–N5	75.39(6)	81.044	5.648	0.0749
O3–Fe1–N9	75.39(6)	82.079	6.683	0.0887
O1–C1–N2	121.7(2)	121.062	0.658	0.0054
O2–C2–N6	121.31(2)	120.697	0.615	0.0051
O3–C3–N10	121.4(2)	120.781	0.531	0.0044
C1–N3–N4	119.5(2)	119.506	0.014	0.0001
C2–N7-–N8	118.53(19)	118.374	0.158	0.0014
C3–N11–N12	119.7(2)	119.257	0.463	0.0039
MAE: 2.3056	SE: 3.5507	MRE: 0.0292		

AE: absolute error; RE: relative error; MAE: mean absolute error; SE: standard error; MRE: mean relative error

The frontier orbital diagrams of the highest occupied molecular orbital (HOMO) and the lowest unoccupied molecular orbital (LUMO) of FeCP are displayed in Figure 6. The HOMO and LUMO are mainly related to the metal-ligand bonding orbital and the metal-ligand anti-bonding orbital, respectively. The initial stage of detonation is an electronic excitation process, so the electronic excitation from HOMO to LUMO leads to the breaking of the metal-ligand bond. The energy gap and the experimental impact sensitivity of FeCP are listed in Table 6, together with those of other MCPs [37].

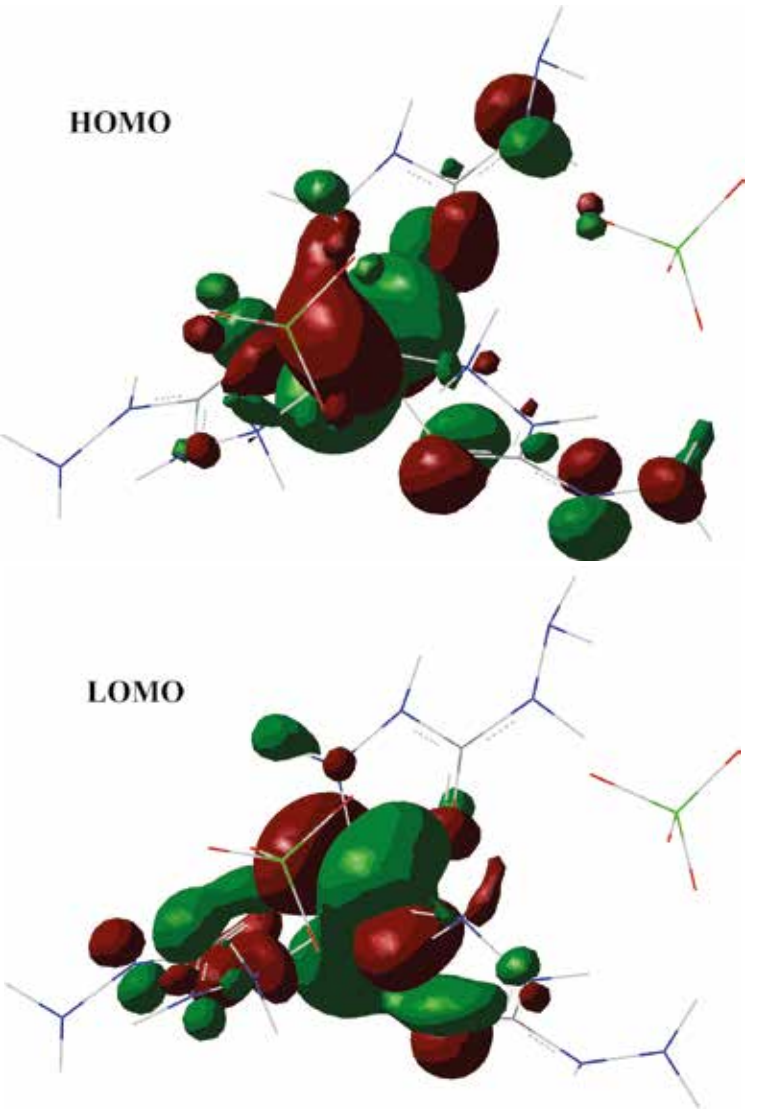

Figure 6. Frontier molecular orbital diagrams of FeCP.

The impact sensitivities of the MCPs (M = Co, Ni, Zn, and Cd) are indeed directly proportional to the energy gap: the smaller energy gap results in the higher impact sensitivity. Previous studies have shown that the band gap is correlated with the impact sensitivity in a solid crystal [52-58]. The initiating reaction of detonation caused by the external mechanical stimulus is an electronic excitation

process. The HOMO and LUMO form the valence band and the conduction band in solids. Therefore, the energy gap between HOMO and LUMO, that is the band gap, is related to the impact sensitivity. The smaller the energy gap is, the easier the electron transfers from the HOMO to the LUMO, and the easier the energetic molecule explosively decomposes.

Conclusions

The crystal configuration of FeCP is a six-coordinated, non-centrosymmetric octahedron. The thermal analysis and sensitivity tests showed that FeCP is less stable and more sensitive to external stimuli than other MCPs and even some other widely-used primary explosives, although FeCP has a relatively high explosive energy due to its high combustion enthalpy. DFT was used to calculate the optimized geometry and the frontier molecular orbitals of FeCP. It was found that the microscopic energy gap between HOMO and LUMO is closely linked with the macroscopic impact sensitivity. The smaller calculated energy gap leads to the higher experimental impact sensitivity. FeCP's very small energy gap is the primary cause for its high sensitivity. This discovery encourages further study of the inherent mechanisms of sensitivity for energetic materials. Although the high sensitivity of FeCP may present challenges for its further applications, the proof of its existence enriches the range of carbohydrazide-based energetic compounds, and also prompts us to pay attention to the safe applications of iron and its compounds.

Appendix

The cif file of FeCP (CCDC number: 788841) was deposited in Cambridge Crystallographic Data Centre. Further details can be obtained free of charge via www.ccdc.cam.ac.uk/conts/retrieving.html (or from the Cambridge Crystallographic Data Centre, 12 Union Road, Cambridge CB21EZ, UK; Fax: + 44 1223 336033).

Acknowledgements

This project was supported by the Science and Technology Fund on Applied Physical Chemistry Laboratory (Nos. 9140C3703051105 and 9140C370303120C37142), and the Key Support Foundation of State Key Laboratory of Explosion Science and Technology (Nos. QNKT12-02 and YBKT 10-05).

References

[1] Wu D., Zheng P., Chang P.R., Ma X., Preparation and Characterization of Magnetic Rectorite/Iron Oxide Nanocomposites and Its Application for the Removal of the Dyes, *Chem. Eng. J.,* **2011**, *174*, 489-494.

[2] Vinita M., Dorathi R.P.J., Palanivelu K., Degradation of 2,4,6-Trichlorophenol by Photo Fenton's Like Method Using Nano Heterogeneous Catalytic Ferric Ion, *Sol. Energy*, **2010**, *84*, 1613-1618.

[3] Wei H., Insin N., Lee J., Han H.-S., Cordero J.M., Liu W., Bawendi M.G., Compact Zwitterion-Coated Iron Oxide Nanoparticles for Biological Applications, *Nano Lett.*, **2012**, *12*, 22-25.

[4] Costo R., Bello V., Robic C., Port M., Marco J.F., Puerto Morales M., Veintemillas-Verdaguer S., Ultrasmall Iron Oxide Nanoparticles for Biomedical Applications: Improving the Colloidal and Magnetic Properties, *Langmuir*, **2012**, *28*, 178-185.

[5] Grimes C.N., Giori L., Fry M.M., Role of Hepcidin in Iron Metabolism and Potential Clinical Applications, *The Veterinary Clinics of North America. Small Animal Pract.*, **2012**, *42*, 85-96.

[6] Okoli C., Fornara A., Qin J., Toprak M.S., Dalhammar G., Muhammed M., Rajarao G.K., Characterization of Superparamagnetic Iron Oxide Nanoparticles and Its Application in Protein Purification, *J. Nanosci. Nanotechno.*, **2011**, *11*, 10201-10206.

[7] Okoli C., Boutonnet M., Mariey L., Jaras S., Rajarao G., Application of Magnetic Iron Oxide Nanoparticles Prepared from Microemulsions for Protein Purification, *J. Chem. Techno. Biotechno.*, **2011**, *86*, 1386-1393.

[8] Huynh M.H.V., Hiskey M.A., Meyer T.J., Wetzler M., Green Primaries: Environmentally Friendly Energetic Complexes, *P. Nat. Acad. Sci.*, **2006**, *103*, 5409-5412.

[9] Huynh M.H.V., Coburn M.D., Meyer T.J., Wetzler M., Green Primary Explosives: 5-Nitrotetrazolato-N_2-ferrate Hierarchies, *P. Nat. Acad. Sci.*, **2006**,103, 10322-10327.

[10] Klapötke T.M., Steinhauser G., "Green" Pyrotechnics: a Chemists' Challenge, *Angew. Chem. Int. Ed.*, **2008**, *47*, 3330-3347.

[11] Talawar M.B., Sivabalan R., Mukundan T., Muthurajan H., Sikder A.K., Gandhe B.R., Rao A.S., Environmentally Compatible Next Generation Green Energetic Materials (GEMs), *J. Hazard. Mater.*, **2009**, *161*, 589-607.

[12] Sinditskii V.P., Fogelzang A.E., Dutov M.D., Sokol V.I., Serushkin V.V., Svetlov B.S., Poraikoshits M.A., Structure of Complex-Compounds of Metal Chlorides, Sulfates, Nitrates and Perchlorates with Carbohydrazine, *Zhurnal Neorganicheskoi Khimii*, **1987**, *32*, 1944-1949.

[13] Talawar M.B., Agrawal A.P., Chhabra J.S., Asthana S.N., Studies on Lead-Free Initiators: Synthesis, Characterization and Performance Evaluation of Transition Metal Complexes of Carbohydrazide, *J. Hazard. Mater.*, **2004**, *113*, 57-65.

[14] Bushuyev O.S., Arguelles F.A., Brown P., Weeks B.L., Hope-Weeks L.J., New

Energetic Complexes of Copper(II) and the Acetone Carbohydrazide Schiff Base as Potential Flame Colorants for Pyrotechnic Mixtures, *Eur. J. Inorg. Chem.*, **2011**, *29*, 4622-4625.

[15] Ilyushin M.A., Tselinskiy I.V., Smirnov A.V., Shugalei I.V., Physicochemical Properties and Laser Initiation of a Copper Perchlorate Complex with 3(5)-Hydrazino-4-amino-1,2,4-triazole (HATr) as a Ligand, *Cent. Eur. J. Energ. Mater.*, **2012**, *9*(1), 3-16.

[16] Cudzilo S., Trzcinski W., Nita M., Michalik S., Krompiec S., Kruszynski R., Kusz J., Preparation, Crystal Structure and Explosive Properties of Copper(II) Perchlorate Complex with 4-Amino-1,2,4-Triazole and Water, *Propellants Explos. Pyrotech.*, **2011**, *36*, 151-159.

[17] Oxley J.C., Smith J.L., Higgins C., Bowden P., Moran J., Brady J., Aziz C.E., Cox E., Efficiency of Perchlorate Consumption in Road Flares, Propellants and Explosives, *J. Environ. Manag.*, **2009**, *90*, 3629-3634.

[18] Koch E.C., Pyrotechnic Countermeasures: II. Advanced Aerial Infrared Countermeasures, *Propellants Explos. Pyrotech.*, **2006**, *31*, 3-19.

[19] Raj A.J.R., Muruganandam L., Batch Studies and Effect of Environmental Parameters on Microbial Degradation of Perchlorate Using Acclimatized Effluent Sludge, *Res. J. Chem. Environ.*, **2012**, *16*, 44-50.

[20] Parker D.R., Perchlorate in the Environment: the Emerging Emphasis on Natural Occurrence, *Environ. Chem.*, **2009**, 6, 10-27.

[21] Lewis W.K., Harruff B.A., Gord J.R., Rosenberger A.T., Sexton T.M., Guliants E.A., Bunker C.E., Chemical Dynamics of Aluminum Nanoparticles in Ammonium Nitrate and Ammonium Perchlorate Matrices: Enhanced Reactivity of Organically Capped Aluminum, *J. Phys. Chem. C*, **2011**, *115*, 70-77.

[22] Khrapovskii V.E., Khudaverdiev V.G., Sulimov A.A., On Convective Combustion of Ammonium Perchlorate Mixtures with Aluminum, *Combust. Explos. Shock Waves (Engl. Transl.)*, **2011**, *47*, 483-489.

[23] Talawar M.B., Agrawal A.P., Chhabra J.S., Ghatak C.K., Asthana S.N., Rao K.U.B., Studies on Nickel Hydrazinium Nitrate (NHN) and bis-(5-Nitro-2H-tetrazolato-N-2) tetraamino Cobalt(III) Perchlorate (BNCP): Potential Lead-Free Advanced Primary Explosives, *J. Sci. Ind. Res.*, **2004**, *63*, 677-681.

[24] Li Z.M., Zhang T.L., Yang L., Zhou Z.N., Zhang J.G., Synthesis, Crystal Structure, Thermal Decomposition, and Non-Isothermal Reaction Kinetic Analysis of an Energetic Complex: Mg(CHZ)(3) (ClO4)(2) (CHZ = Carbohydrazide), *J. Coord. Chem.*, **2012**, *65*, 143-155.

[25] Qi S.Y., Li Z.M., Zhang T.L., Zhou Z.N., Yang L., Zhang J.G., Qiao X.J., Yu K.B., Crystal Structure, Thermal Analysis and Sensitivity Property of $[Zn(CHZ)_3](ClO_4)_2$, *Acta Chim. Sinica*, **2011**, *69*, 987-992.

[26] Huang H.S., Zhang T.L., Zhang J.G., Wang L.Q., A Screened Hybrid Density Functional Study on Energetic Complexes: Cobalt, Nickel and Copper Carbohydrazide Perchlorates., *J. Hazard. Mater.*, **2010**, *179*, 21-27.

[27] Sun Y.H., Zhang T.L., Zhang J.G., Yang L., Qiao X.J., Decomposition Kinetics of

Manganese tris (Carbohydrazide) Perchlorate (MnCP) Derived from the Filament Control Voltage of the T-jump/FTIR Spectroscopy, *Int. J. Therm. Sci.*, **2006**, *45*, 814-818.

[28] Sun Y.H., Zhang T.L., Zhang J.G., Yang L., Qiao X.J., Kinetics of Flash Pyrolysis of $Co(CHZ)_3$ $(ClO_4)_2$ and $Ni(CHZ)_3ClO_4)_2$, *Acta Phys.-Chim. Sinica*, **200**6, *22*, 649-652.

[29] Sun Y.H., Zhang T.L., Zhang J.G., Qiao X.J., Yang L., Flash Pyrolysis Study of Zinc Carbohydrazide Perchlorate Using T-jump/FTIR Spectroscopy, *Combust. Flame*, **2006,** *145*, 643-646.

[30] Klapötke T.M., Stierstorfer J., The CN_7^- Anion, *J. Am. Chem. Soc.*, **2009**, *131*,1122-1134.

[31] Huynh M.H.V., Hiskey M.A., Chavez D.E., Naud D.L., Gilardi R.D., Synthesis, Characterization, and Energetic Properties of Diazido Heteroaromatic High-Nitrogen C-N Compound, *J. Am. Chem. Soc.*, **2005**, *127*, 12537-12543.

[32] Carlqvist P., Ostmark H., Brinck T., The Stability of Arylpentazoles, *J. Phys. Chem A*, **2004**, *108*, 7463-7467.

[33] Sheldrick G.M., *SHELXS-97, Program for the Solution of Crystal Structure*, Germany: University of Göttingen, **1997**.

[34] GJB 5891.22-2006, Test Method of Loading Material for Initiating Explosive Device − Part 22: Mechanical Impact Sensitivity Test, Commission of Science Technology and Industry for National Defense, **2006**, 131-135.

[35] GJB 5891.24-2006, Test Method of Loading Material for Initiating Explosive Device − Part 24: Friction Sensitivity Test, Commission of Science Technology and Industry for National Defense, **2006**, 143-147.

[36] GJB 5891.25-2006, Test Method of Loading Material for Initiating Explosive Device − Part 25: Sensitivity to Flame Test, Commission of Science Technology and Industry for National Defense, **2006**, 151-153.

[37] Huang H.S., Zhang T.L., Zhang J.G., Wang L.Q., Density Functional Theoretical Study of Transition Metal Carbohydrazide Perchlorate Complexes, *Chem. Phys. Lett.*, **2010**, *487*, 200-203.

[38] Zhang T.L., Hu R.Z., Xie Y., Li F.P., The Estimation of Critical-Temperatures of Thermal-Explosion for Energetic Materials Using Nonisothermal DSC., *Thermochim. Acta*, **1994**, *244*, 171-176.

[39] Hu R.Z., Ning B.K., Yu Q.S., Zhang T.L., Liu R., Yang Z.Q., Gao S.L., Zhao H.A., Shi Q.Z., Estimation of the Critical Temperature of Thermal Explosion for Energetic Materials Using Non-Isothermal Analysis Method, *Chin. J. Energ. Mater*, **2003**, *11*, 18-25.

[40] Ou Y.X. *Explosives*, Beijing: Beijing Institute of Technology Press, **2006**.

[41] Lv C.H., Zhang T.L., Ren B.L., Yu K.B., Lu Z., Cai R.J., Preparation, Structure, and Explosive Properties of $[Co(CHZ)_3](ClO_4)_2$, *Chin. J. Explos.,* **2000**, *1*, 31-33.

[42] Zhang J.G., Zhang T.L., Wei Z.R., Yu K.B., Studies on Preparation, Crystal Structure and Application of $Mn(CHZ)_3$ $(ClO_4)_2$, *Chem. J. Chin. Univ.-Chin.*, **2001**, *22*, 895-897.

[43] Huynh M.H.V., Hiskey M.A., Hartline E.L., Montoya D.P., Gilardi R., Polyazido High-Nitrogen Compounds: Hydrazo- and Azo-1,3,5-triazine, *Angew. Chem. Int. Ed.*, **2004**, *43*, 924-4928.

[44] Talawar M.B., Agrawal A.P., Asthana S.N., Energetic Co-ordination Compounds: Synthesis, Characterization and Thermolysis Studies on bis-(5-Nitro-2H-tetrazolato-N-2)tetraammine Cobalt(III) Perchlorate (BNCP) and Its New Transition Metal (Ni/Cu/Zn) Perchlorate Analogues, *J. Hazard. Mater.*, **2005**, *120*, 25-35.

[45] Lai W.P., Lian P., Wang B.Z., Ge Z.X., New Correlations for Predicting Impact Sensitivities of Nitro Energetic Compounds, *J. Energ. Mater.*, **2010**, *28*, 45-76.

[46] Badders N.R., Wei C., Aldeeb A.A., Rogers W.J., Mannan M.S., Predicting the Impact Sensitivities of Polynitro Compounds Using Quantum Chemical Descriptors, *J. Energ. Mater.*, **2006**, *24*, 17-33.

[47] Ramaswamy A.L., Mesoscopic Approach to Energetic Material Sensitivity, *J. Energ. Mater.*, 2006, *24*, 35-65.

[48] Gilman J.J., Bond Modulus and Stability of Covalent Solids, *Philos. Mag. Lett.*, **2007**, *87*,121-124.

[49] Gilman J.J., *Mechanochemical Mechanisms in Stress Corrosion,* Chemistry and Electrochemistry of Corrosion and Stress Corrosion Cracking: A Symposium Honoring the Contributions of R.W. Staehle (Jones R.H., Ed.) **2001**.

[50] Gilman J.J., Chemical and Physical "Hardness", *Mater. Res. Innov.*, **1997**, 1, 71-76.

[51] Gilman J.J., Chemical-Reactions at Detonation Fronts in Solids, *Philos. Mag. B*, **1995**, *71*, 1057-1068.

[52] Chen F., Cheng X.L., A First-Principles Investigation of the Hydrogen Bond Interaction and the Sensitive Characters in cis-1,3,4,6-Tetranitrooctahydroimidazo-4,5-dimidazole, *Int. J. Quantum Chem.*, **2011**, *111*, 4457-4464.

[53] Li J., Relationships for the Impact Sensitivities of Energetic C-Nitro Compounds Based on Bond Dissociation Energy, *J. Phys. Chem. B*, **2010**, 114, 2198-2202.

[54] Zhu W., Xiao H., First-Principles Study of Electronic Structure, Absorption Spectra, and Thermodynamic Properties of Crystalline 1H-Tetrazole and Its Substituted Derivatives, *Structural Chemistry*, **2010**, *21*, 847-854.

[55] Wang G.X., Gong X.D., Xiao H.M., A Theoretical Investigation on Pyrolysis Mechanism and Impact Sensitivity of Nitro Derivatives of Benzene and Aminobenzenes, *Acta Chim. Sinica*, **2008**, *66*, 711-716.

[56] Zhang H., Cheung F., Zhao F., Cheng X.L., Band Gaps and the Possible Effect on Impact Sensitivity for Some Nitro Aromatic Explosive Materials, *Int. J. Quantum Chem.*, **2009**, *109*, 1547-1552.

[57] Zhu W., Xiao H., First-Principles Study of Electronic, Absorption, and Thermodynamic Properties of Crystalline Styphnic Acid and Its Metal Salts, *J. Phys. Chem. B*, **2009**, *113*, 10315-10321.

[58] Zhu W., Zhang X., Wei T., Xiao H., First-principles Study of Crystalline Mono-Amino-2,4,6-trinitrobenzene, 1,3-Diamino-2,4,6-trinitrobenzene, and 1,3,5-Triamino-2,4,6-trinitrobenzene, *J. Mol. Struc.-Theochem.*, **2009**, *900*, 84-89.